Temperature Dependent Calculations of Optical Potential in Elastic Scattering Cross Section Basis: An Application to $^{10}B + ^{120}Sn$ Reaction

MURAT AYGÜN[1*]

[1] *Department of Physics, Bitlis Eren University, Bitlis 13000, Turkey*

Abstract

We examine the effect of temperature on the elastic scattering angular distributions of $^{10}B + ^{120}Sn$ reaction. For this, we use two-parameter fermi density distribution for both ^{10}B and ^{120}Sn nuclei as a function of temperature (T = 0, 1, 2, 3, 4, 5, 6, 7 MeV). We obtain the real potentials by using these density distributions within the double folding model based on the optical model. The imaginary part of the optical potential is considered as Woods-Saxon potential. We calculate the elastic scattering angular distributions for all the investigated cases. To see differences between the theoretical results, we compare our results with the experimental data. Then, we discuss the relationship between different root mean square (rms) radii of the nuclei. Finally, we give volume integrals and cross sections according to various temperature values.

Keywords: Density distribution, nuclear potential, optical model

Introduction

As the temperature of a nucleus increases, its density distribution changes. This result has been shown within Hartree-Fock calculations (Brack and Quentin (1974); Mosel et al., (1974); Quentin and Flocard (1978); La Rana et al., (1984)). This change in density distribution causes a change in the potential that is used to describe an interacting system. Therefore, it is easier to explain the interacting system if nuclear potential is properly identified.

The optical model that consists of real and imaginary potentials is one of an effective models in identifying nuclear potential of interacting two nuclei. For the calculations of real and imaginary potentials, a microscopical or phenomenological analysis can be preferred (Aygun (2015); Aygun (2018)). In this respect, the double folding model based on the optical model is a microscopical approach that depends on density distributions of the interacting nuclei. The double folding potential is obtained at zero temperature in general. However, it is assumed that the density of a heated nucleus changes. Thus, the temperature dependence of the optical potential may be due to the temperature dependence of density distributions (Guo-Qiang and Gong-Ou (1990)). The temperature dependence of interaction potential was examined previously (Bandyopadhyay et al., (1992)). It was noticed that the fusion barrier decreases as the temperature increases. As a result of this, the nuclear potential that defines a system can need some corrections (Osman and Abdel-Aziz (1990)). The inclusion of this effect can also allow for the variations that may occur due to the temperature dependence of any system. An important application of such a search is to see the influence of the temperature on the elastic scattering.

Recently, Gasques et al. (2018) have measured the elastic, inelastic and 1n transfer cross sections of $^{10}B + ^{120}Sn$ reaction at incident energy of E_{Lab} = 37.5 MeV. They have performed an analysis of the theoretical treatment with the experimental data. In this respect, they have applied one-step distorted-wave Born approximation (DWBA) and coupled reaction

Received: 25.03.2019
Revised: 10.05.2019
Accepted:15.05.2019
[*]*Corresponding author: Murat Aygün, PhD*
Department of Physics, Bitlis Eren University, Bitlis 13000, Turkey
E-mail: murata.25@gmail.com
Cite this article as: M. Aygün, Temperature Dependent Calculations of Optical Potential in Elastic Scattering Cross Section Basis: An Application to $^{10}B + ^{120}Sn$ Reaction, *Eastern Anatolian Journal of Science, Vol. 5, Issue 1, 33-42, 2019*

channels (CRC) calculations via the double folding São Paulo potential. As a result of the elastic scattering cross section of this study (Gasques et al., (2018)), the idea of using a different approach for the computation of the nuclear potential is appear. Thus, we propose to examine the temperature dependent effect of density distribution in calculating the real part of the optical potential.

In the present work, we investigate the temperature dependence of the optical potential. In order to do this search, we perform temperature dependent calculations of the elastic scattering angular distributions of ^{10}B + ^{120}Sn reaction by using a temperature dependent density distribution like two-parameter Fermi type (2pF) for both ^{10}B and ^{120}Sn nuclei. For this, first of all, we apply T = 0 case of the 2pF density distribution. Then, we obtain the density distributions of ^{10}B and ^{120}Sn nuclei at temperatures T = 1, 2, 3, 4, 5, 6, 7 MeV. Then, we calculate the elastic scattering cross sections by means of double folding model based on the optical model and compare our results with the experimental data.

In section II, we define the theoretical approach and calculations for temperature dependent and temperature independent density distributions. In section III, we give the results and discussions. Finally, we provide the conclusions in section IV.

2. Theoretical Process

The interaction potential that is evaluated in the theoretical calculations can be written as

$$U(r) = V_{Coulomb}(r) + \underbrace{V_{Nuclear}(r)}_{\underbrace{V(r)}_{\text{Real Part}} + \underbrace{iW(r)}_{\text{Imaginary Part}}} \tag{1}$$

$V_{Coulomb}(r)$ potential is shown by (Satchler (1983))

$$V_{Coulomb}(r) = \begin{cases} \frac{1}{4\pi\varepsilon_0}\frac{Z_P Z_T e^2}{r}, & r \geq R_C \quad (2) \\ \frac{1}{4\pi\varepsilon_0}\frac{Z_P Z_T e^2}{2R_C}\left(3 - \frac{r^2}{R_C^2}\right), & r < R_C \quad (3) \end{cases}$$

$$R_c = 1.25\left(A_P^{1/3} + A_T^{1/3}\right) \tag{4}$$

where R_c is the Coulomb radius, and Z_P (Z_T) denotes the charge of projectile (target) nucleus, respectively. The nuclear potential can be obtained by using the optical model which is one of the most important models used extensively to describe the scattering cross sections of both light-ion and heavy-ion reactions. The double folding model, evaluated in our calculations, is one of the most useful microscopical models applied to determine the real potential. The double folding potential that uses the density distributions of projectile and target nuclei together with an effective nucleon-nucleon interaction potential (v_{NN}) is parameterized as

$$V_{\mathrm{DF}}(\boldsymbol{r}) = \int d\boldsymbol{r_1} \int d\boldsymbol{r_2} \rho_P(\boldsymbol{r_1}) \rho_T(\boldsymbol{r_2})\, v_{NN}(r_{12}), \tag{5}$$

where $\rho_P(\boldsymbol{r_1})$ and $\rho_T(\boldsymbol{r_2})$ denote the densities of projectile and target nuclei, respectively. In general, the double folding calculations are applied at zero temperature. However, we examine both temperature dependent and temperature independent changes of the double folding potential with this study. For this purpose, we consider 2pF density distribution for different temperatures shown by (Gupta et al., (2007))

$$\rho_i(r) = \frac{\rho_{0i}(T)}{[1+\exp\left(\frac{r-R_{0i}(T)}{a_i(T)}\right)]}, \quad (6)$$

where the central density, ρ_{0i}, is written as

$$\rho_{0i}(T) = \frac{3A_i}{4\pi R_{0i}^3(T)}[1 + \frac{\pi^2 a_i^2(T)}{R_{0i}^2(T)}]^{-1}, \quad (7)$$

the half-density radius, $R_{0i}(T = 0)$, is given by

$$R_{0i}(T = 0) = 0.90106 + 0.10957A_i - 0.0013A_i^2 + 7.71458 \times 10^{-6}A_i^3 - 1.62164 \times 10^{-8}A_i^4, \quad (8)$$

and the surface thickness parameter, $a_i(T = 0)$, is parameterized as

$$a_i(T = 0) = 0.34175 + 0.01234A_i - 2.1864 \times 10^{-4}A_i^2 + 1.46388 \times 10^{-6}A_i^3 - 3.24263 \times 10^{-9}A_i^4. \quad (9)$$

In order to calculate the real part of the nuclear potential at different temperatures, we apply temperature dependent forms of $R_{0i}(T)$ and $a_i(T)$ parameters shown by (Shlomo and Natowitz (1991))

$$R_{0i}(T) = R_{0i}(T = 0)[1 + 0.0005T^2], \quad (10)$$

$$a_i(T) = a_i(T = 0)[1 + 0.01T^2]. \quad (11)$$

The type of v_{NN} is assumed in the following form

$$v_{NN}(r) = 7999\frac{\exp(-4r)}{4r} - 2134\frac{\exp(-2.5r)}{2.5r} + J_{00}(E)\delta(r)(MeV), \quad (12)$$

where $J_{00}(E)$, the exchange term, is

$$J_{00}(E) = 276\left[1 - \frac{0.005E_{\mathrm{Lab}}}{A_P}\right] MeVfm^3 \quad (13)$$

The imaginary part of the optical potential is taken as the Woods-Saxon potential within the phenomenological approach.

$$W(r) = -\frac{W_0}{1+\exp\left(\frac{r-R_W}{a_W}\right)} \quad (14)$$

where $R_w = r_w (A_P^{1/3} + A_T^{1/3})$, W_0 is the imaginary depth, r_w is the radius parameter and $A_P(A_T)$ is the mass number of projectile(target) nucleus, respectively. The theoretical results are acquired by using the code FRESCO (Thompson (1988)). However, the double folding calculations are performed by the help of code DFPOT (Cook (1982)).

3. Results and Discussion

We have determined the optical potential parameters to calculate the elastic scattering cross sections of ^{10}B + ^{120}Sn reaction as a function of temperature. With this aim, we have first fixed to unity the renormalization factor (N_R) of the real potential based on the double folding model calculations. Then, we have examined the parameters (W_0, r_w, a_w) of the imaginary potential in order to achieve good agreement results with the experimental data. We have searched r_w and a_w parameters in steps of 0.1 and 0.01 fm and have fixed at 1.17 fm and 0.55 fm values, respectively. Finally, we have defined the W_0 values that are listed in Table I.

Table I: The optical potential parameters, real and imaginary volume integrals (in MeV.fm^3) and cross sections (mb) determined in the analysis of the elastic scattering angular distributions for 2pF densities of ^{10}B and ^{120}Sn nuclei at various temperatures (T = 0, 1, 2, 3, 4, 5, 6, 7 MeV). In all the calculations, r_w = 1.31 fm and a_w = 0.558 fm.

Nucleus	T (MeV)	W_0 (MeV)	J_v ($MeV.fm^3$)	J_w ($MeV.fm^3$)	σ (mb)
^{10}B	0	30.4	414.7	87.9	458.1
	1	30.4	414.8	87.9	459.2
	2	24.0	414.8	69.4	424.3
	3	17.7	415.0	51.2	387.3
	4	12.7	415.2	36.7	359.8
	5	8.00	415.6	23.1	340.1
	6	6.00	416.2	17.3	360.8
	7	5.00	417.1	14.4	409.8
^{120}Sn	0	30.4	414.7	87.9	458.1
	1	26.0	414.7	75.2	433.8
	2	22.0	414.7	63.6	413.5
	3	16.0	414.8	46.2	381.1
	4	11.0	414.8	31.8	361.5
	5	10.0	414.8	28.9	391.9
	6	6.00	414.8	17.3	419.9
	7	6.00	414.9	17.3	506.3
Both	0	30.4	414.7	87.9	458.1
	1	27.0	414.8	78.1	441.2
	2	18.0	414.8	52.0	390.5
	3	11.0	415.0	31.8	356.4
	4	9.00	415.2	26.0	386.5
	5	7.80	415.6	22.5	453.9
	6	6.80	416.3	19.6	558.3
	7	5.80	417.2	16.7	700.6

Figure 1 shows the variations with the distance of temperature independent and temperature dependent 2pF densities of ^{10}B projectile and ^{120}Sn target nucleus. In this context, Fig. 1 (a) displays temperature independent 2pF densities of ^{10}B and ^{120}Sn nuclei at T = 0 MeV, Fig. 1 (b) and (c) present temperature dependent 2pF densities of ^{10}B and ^{120}Sn at T = 1, 2, 3, 4, 5, 6, 7 MeV, respectively. It is seen from Fig. 1 (b) and (c) that the central density of ^{10}B and ^{120}Sn nuclei decreases with increasing the temperature. The amount of this decrease becomes the more distinct as the temperature increases. On the other hand, it is observed that the tail parts of the density distributions extend with the increase in temperature. That is, the surface regions of the densities are broadened. This case causes both the increase of root mean square (rms) and the change of nuclear potential.

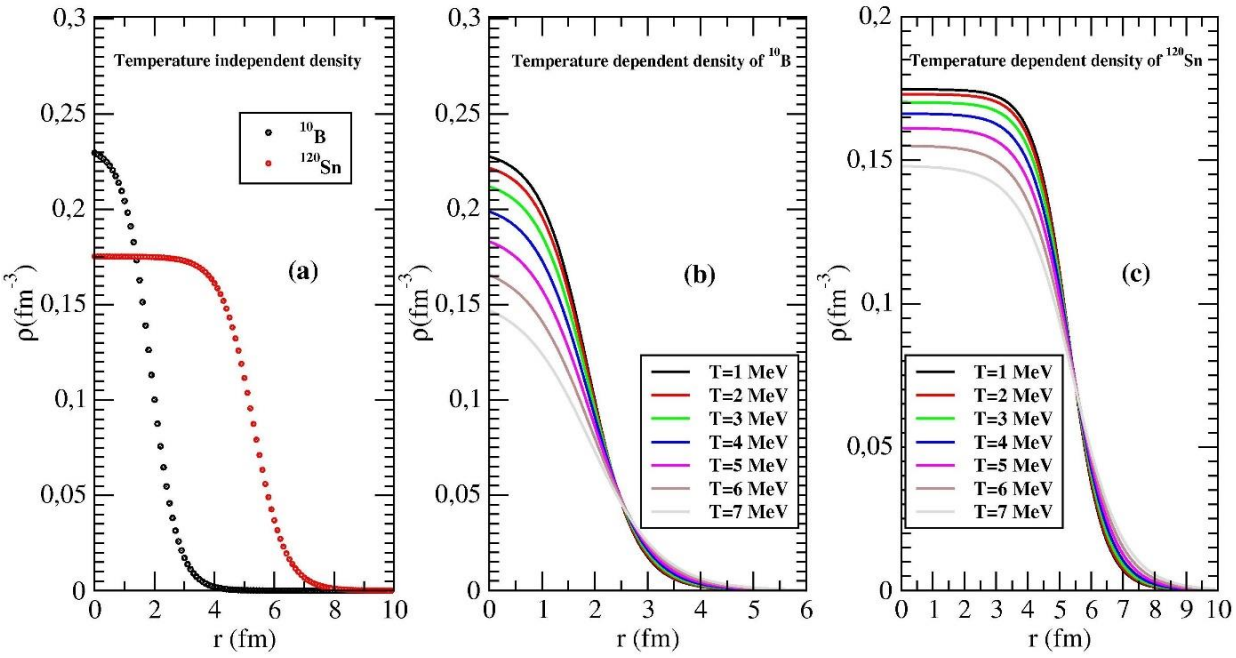

Figure 1. Density distributions as a function of r (fm) of (a) the ^{10}B and ^{120}Sn nuclei at T= 0 MeV, (b) the ^{10}B nucleus at T = 1, 2, 3, 4, 5, 6, 7 MeV, and (c) the ^{120}Sn nucleus at T = 1, 2, 3, 4, 5, 6, 7 MeV.

Figure 2 exhibits the variations with the temperature of the rms values of ^{10}B and ^{120}Sn nuclei at T = 0, 1, 2, 3, 4, 5, 6, 7 MeV. It is realized that the rms values of ^{10}B and ^{120}Sn nuclei increase as a function of the temperature. This situation can be considered as the outward shift of nucleon density distributions (Guo-Qiang and Gong-Ou (1990)).

We have also calculated the elastic scattering cross sections by using both temperature dependent and temperature independent 2pF densities of ^{10}B projectile from T = 0 to T = 7 MeV. At this stage the density distribution of the 120Sn target nucleus is considered to be independent of temperature. Then, we compare our results with the experimental data in Fig. 3. The results of T = 0 MeV and T = 1 MeV are almost identical to each other, but the differences in the results are more pronounced at the next temperatures. At T = 3 MeV, the theoretical results are in better agreement with the data compared to all the other T-values. At higher temperatures (T > 4 MeV), the results are not good enough. That is, if the temperature of the density distribution of ^{10}B nucleus is increased, agreement results with experimental data can not be reproduced adequately. Therefore, we do not perform the calculations at much higher temperatures where nuclei can be unstable for both clustering and fragmentation cases (Guo-Qiang and Gong-Ou (1990)).

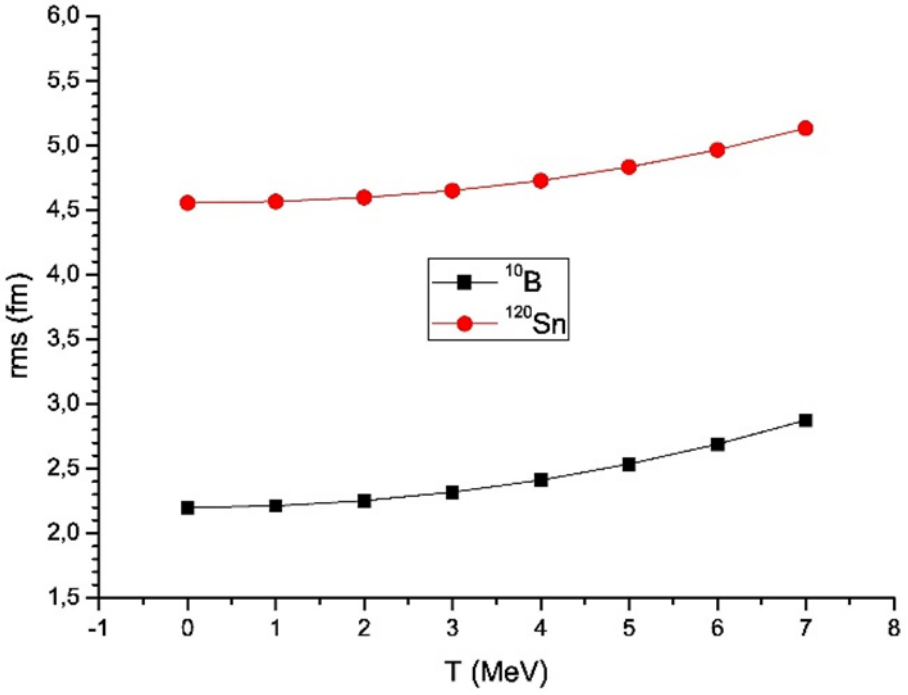

Figure 2. The rms radii of the ^{10}B and ^{120}Sn nuclei as function of temperature.

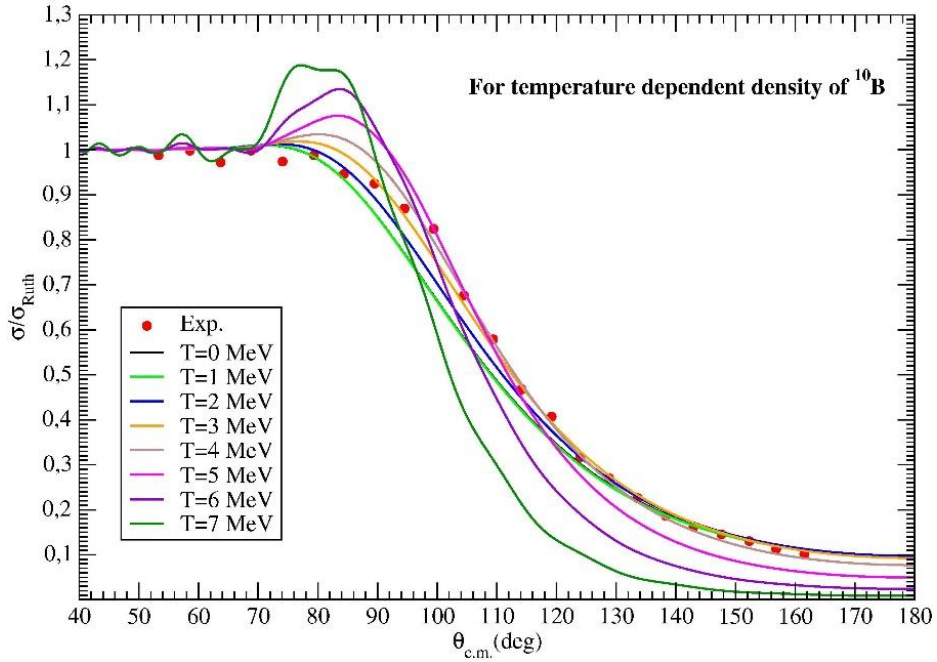

Figure 3. The elastic scattering angular distributions of ^{10}B + ^{120}Sn reaction for 2pF density of the ^{10}B nucleus at T = 0, 1, 2, 3, 4, 5, 6, 7 MeV. The experimental data is obtained from Ref. Gasques et al. (2018).

We calculate the elastic scattering cross sections of ^{10}B + ^{120}Sn reaction by using 2pF density based on different temperatures of ^{120}Sn target nucleus. For this case, the density of ^{10}B projectile is independent of temperature. We present as compared the theoretical results with the experimental data in Fig. 4. We obtain the best results for T = 3 MeV. We also observe that our results describe very well the experimental data.

We realize that the results are similar to the results of previous analysis.

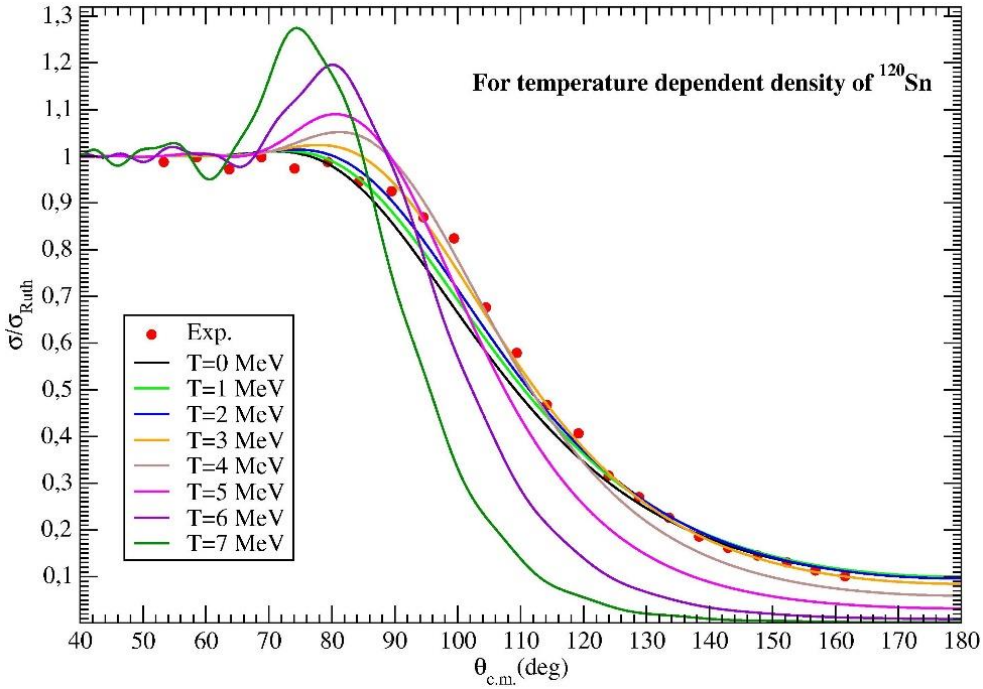

Figure 4. The same as Fig. 3, but for the ^{120}Sn nucleus.

In our work, we try to investigate the temperature related changes of the density distributions of ^{10}B and ^{120}Sn nuclei simultaneously. For this purpose, we acquire the elastic scattering angular distributions of $^{10}B + ^{120}Sn$ system at T = 0, 1, 2, 3, 4, 5, 6, 7 MeV. Then, we compare all the theoretical results with the experimental data in Fig. 5. We observe that the results for T = 2 MeV are better than the results of the other temperatures and are in good agreement with the experimental data. Additionally, we notice that the theoretical results are far from the harmony with the data at high temperatures.

In Fig. 6, we compare with each other the best results of the three situations. We first notice that the variation of the density distribution with temperature significantly influences the theoretical results and gives better results than temperature independent results. Secondly, we find that temperature dependent results of ^{10}B nucleus at T = 3 MeV and temperature dependent results of both ^{10}B and ^{120}Sn nuclei at T = 2 MeV are very close to each other and are better than other results. Thus, we can deduce that the variations with temperature of 2pF density distribution have an important impact on the elastic scattering cross sections and increase the agreement between theoretical results and experimental data at a specific energy.

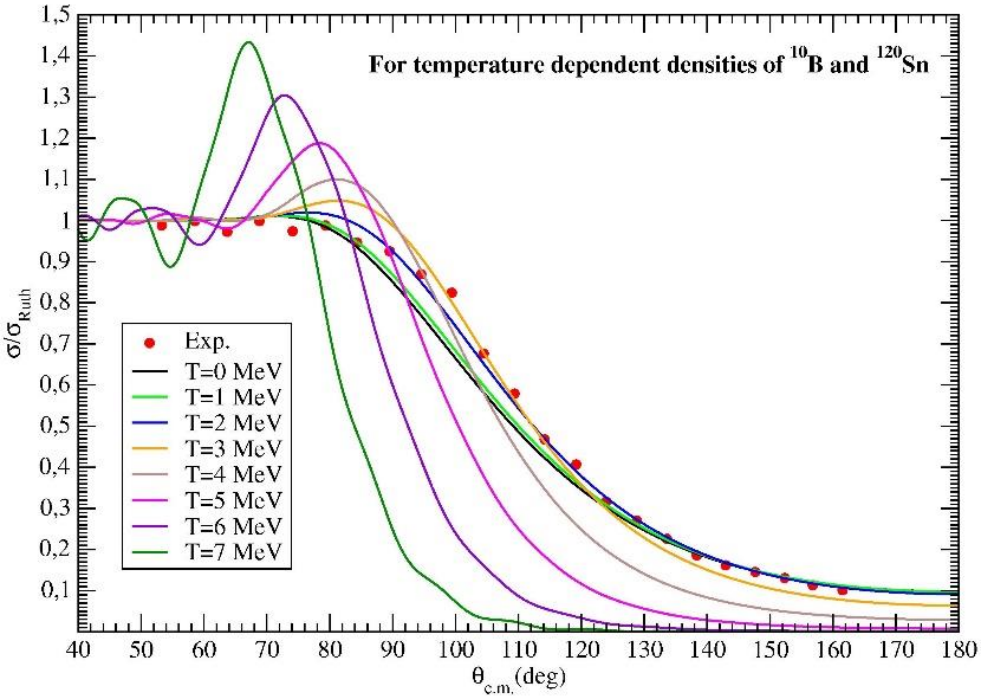

Figure 5. The same as Fig. 3, but for both ^{10}B and ^{120}Sn nuclei.

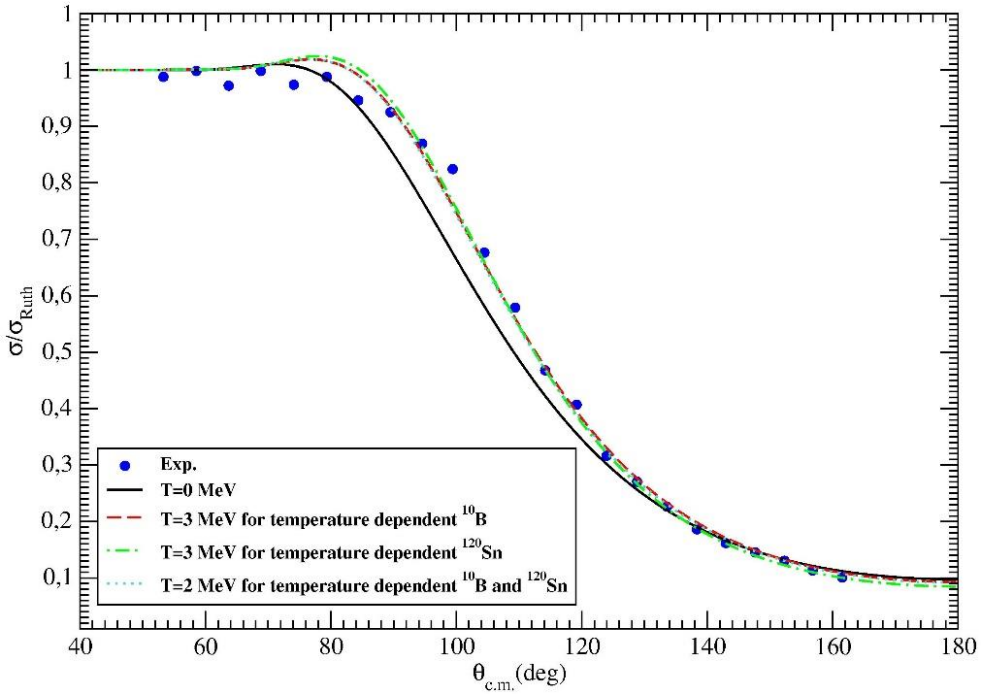

Figure 6. The comparison with each other of the best results of three situations.

In the present study, we also examine the changes with the temperature of the real parts of the nuclear potentials and present as compared the real parts with the distance for T = 0, 1, 2, 3, 4, 5, 6, 7 MeV in Fig. 7. We observe that the real potentials decrease when the temperature increases. Simultaneously, the tails of real potentials extend at larger distances with increasing the temperature. As a result of this, the nuclear potential becomes more attractive.

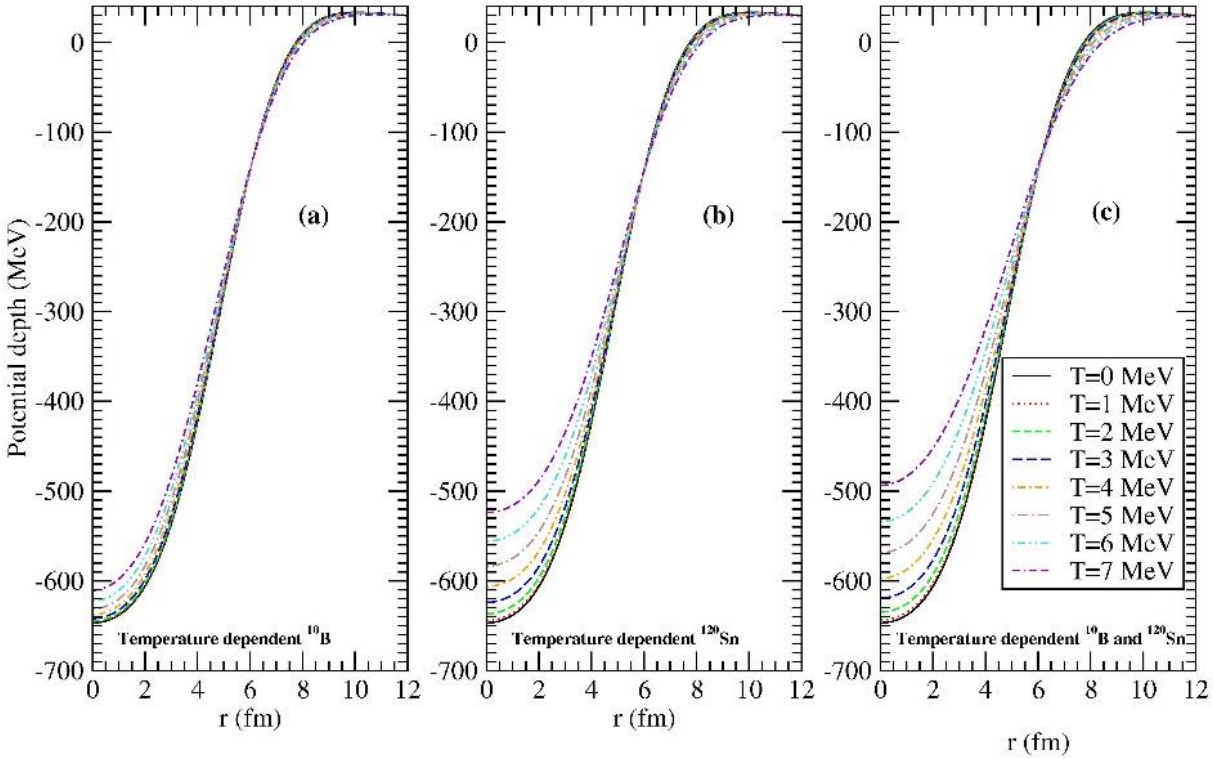

Figure 7. The real potentials as a function of r (fm) at T = 0, 1, 2, 3, 4, 5, 6, 7 MeV of (a) the ^{10}B nucleus, (b) the ^{120}Sn nucleus, and (c) both ^{10}B and ^{120}Sn nuclei.

4. Conclusions

In this paper, we have addressed, for the first time, the calculations of temperature dependent and temperature independent 2pF density distributions of ^{10}B and ^{120}Sn nuclei for the analysis of $^{10}B + ^{120}Sn$ elastic scattering. We have found a good agreement between the experimental data and the temperature dependent results. As a consequence, we can conclude that the temperature dependence density distributions of ^{10}B and ^{120}Sn nuclei will be useful in explaining the elastic scattering results.

References

Brack M., Quentin P. (1974), Selfconsistent calculations of highly excited nuclei. Phys. Lett. B 52: 159.

Mosel U., Zint P. -G., Passler K. H. (1974), Self-consistent calculations for highly excited compound nuclei. Nucl. Phys. A 236: 252.

Quentin P., Flocard H. (1978), Self-consistent calculations of nuclear properties with phenomenological effective forces. Ann. Rev. Nucl. Sci. 28: 523.

La Rana G., Ngô C., Faessler A., Rikus L., Sartor R., Barranco M., Vias X. (1984), Heavy-ion optical potentials at finite temperature calculated using a complex effective interaction derived from a realistic force. Nucl. Phys. A 414: 309-315.

Aygun M. (2018), Alternative potentials analyzing the scattering cross sections of $^{7,9,10,11,12,14}Be$ isotopes from a ^{12}C target: Proximity potentials. J. Korean Phys. Soc. 73, 1255-1262.

Aygun M. (2015), Extended analysis of quasielastic scattering of $^{9}Li + ^{12}C$. J. Korean Phys. Soc. 66, 1816-1821.

Guo-Qiang L., Gong-Ou X. (1990), Optical potential and the fusion barrier of two hot nuclei. Phys. Rev. C 41: 169.

Bandyopadhyay D., Samaddar S. K., Saha R., De J. N. (1992), Fusion limited by temperature. Nucl. Phys. A 539: 370-380.

Osman A., Abdel-Aziz S. S. (1990), Dependence of the interaction potential and fusion cross-section on temperature. Acta Phys. Hung. 67: 367-379.

Gasques L. R., et al. (2018), Elastic, inelastic, and 1n transfer cross sections for the ^{10}B + ^{120}Sn reaction. Phys. Rev. C 97, 034629 (2018).

Satchler G. R. (1983), Direct Nuclear Reactions (Oxford University Press, Oxford).

Gupta R. K., Singh D., Greiner W. (2007), Semiclassical and microscopic calculations of the spin-orbit density part of the Skyrme nucleus-nucleus interaction potential with temperature effects included. Phys. Rev. C 75: 024603.

Shlomo S., Natowitz J. B. (1991), Temperature and mass dependence of level density parameter. Phys. Rev. C 44: 2878.

Thompson I. J. (1988), Coupled reaction channels calculations in nuclear-physics. Comput. Phys. Rep. 7: 167.

Cook J. (1982), DFPOT-a program for the calculation of double folded potentials. Comput. Phys. Commun. 25: 125.